NASA
Technical
Paper
1997

April 1982

Analysis and Monte Carlo Simulation of Near-Terminal Aircraft Flight Paths

James R. Schiess and
Christine G. Matthews

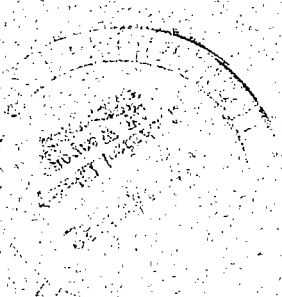

NASA

NASA
Technical
Paper
1997

1982

Analysis and Monte Carlo Simulation of Near-Terminal Aircraft Flight Paths

James R. Schiess
Langley Research Center
Hampton, Virginia

Christine G. Matthews
Computer Sciences Corporation
Hampton, Virginia

National Aeronautics
and Space Administration

**Scientific and Technical
Information Branch**

CONTENTS

INTRODUCTION

Some present-day aeronautics studies center on aircraft flight operations in the airspace surrounding airports. The Aircraft-Noise Levels and Annoyance Model (ref. 1), for example, attempts to quantify the noise impact of airport operations on the surrounding community by combining descriptive information of flight operations with a variety of demographic data about the community. In another study, research is being conducted on the automation of terminal-area flight operations in order to improve overall air traffic capacity and efficiency as well as approach and landing capability during adverse weather conditions (ref. 2).

Any study involving near-terminal flight operations requires an adequate model of aircraft movement along a given trajectory. It is well known, however, that on actual flights there is some dispersion of the individual flight paths along the nominal trajectory. It is necessary to simulate these dispersions within the model in order to accurately assess the effect of actual flight operations.

This paper addresses the problem of stochastically representing the geometry of flight paths of arriving and departing aircraft at a given airport. The flight paths are considered to be joined linear and curvilinear segments. The variables describing these segments are then derived. Statistics of the variables developed from a sample of flight paths are used to select the best fitting distribution from several candidate probability distributions. Conversely, information on the probability distributions of the segment variables are used in a Monte Carlo simulation to generate a random sample of flight paths at the airport. The analysis and simulation techniques presented are illustrated using actual flight paths recorded at Dulles International Airport.

DESCRIPTION OF VARIABLES

The discussion in this section addresses the variables used to describe the aircraft flight paths. The variables are defined, and the procedures required to transform radar tracking data to these variables are outlined.

Data Description

The tracking data available for this study consist of the three-dimensional Cartesian coordinates (x,y,h) of aircraft trajectories relative to a ground-based radar tracking system which records one data point per revolution of the radar antenna. Since an aircraft is usually tracked for several minutes and the radar rotates at a rate of approximately one revolution every 4.5 sec, one flight path is represented by about 300 measurements. Such a large number of measurements for a single flight path would make the process of fitting distributions to many paths complicated and computationally cumbersome.

Segment Representation

The analysis and simulation processes are simplified by defining a more global geometric representation of a single flight path. To accomplish this, each flight path is assumed to consist of alternating linear and curvilinear segments. The segment extending from the end of the runway is always taken to be a linear segment since, during a departure or an approach, the flight path in this area approximately coincides with an imaginary linear extension of the runway. Line segments are described by the three variables: length ℓ, track angle Ψ (measured positively in the clockwise direction from true north), and change in altitude Δh between end points (fig. 1). The curvilinear segments are assumed to be arcs of circles. As such, each is described by the radius of the circle r, the angular measure of the arc θ, and the change in altitude Δh between end points (fig. 1). The ground track, which is the projection of the flight path onto the x-y plane, is defined by ℓ and Ψ for the linear segments and by r and θ for the curvilinear segments. Each linear segment is assumed to be tangent to the adjoining arc in order to achieve a smooth path.

To further limit the number of descriptive variables required, each flight path is restricted to five segments at most. Thus, the path of a single trajectory can be represented by a maximum of 15 variables. In addition, only the nine possible ground tracks illustrated in figure 2 are allowed, since the near-terminal-area air traffic tends to follow certain specified pathways. This means that for an arbitrary airport and runway, segments near the runway (for example, L2) will be heavily represented by data, while segments farther from the runway (such as L7) may not be represented at all. However, the nine allowable ground tracks provide basic patterns one might expect to see near an airport.

Initial Coordinates

The final variables required to describe a flight path fixed in space are the initial coordinates of the trajectory. Given the coordinates of the runway endpoint, the point on the flight path (x,y,h) which is closest to the runway endpoint and exceeds a specified minimum altitude h^* is considered to be the first point on the track. The minimum altitude h^* is a value greater than the runway altitude to ensure the aircraft is airborne. Hence, all data relating to aircraft movement on either taxi aprons or runways are eliminated from the analysis. Furthermore, since runway identification may not be given, locating the closest pair of flight-path and runway-end coordinates also identifies the runway used.

Flight-Path Processing

Given the initial point of the flight path, the Cartesian coordinates are processed sequentially to the outer extremity of the trajectory. The processing consists of grouping the coordinates into alternate linear and curvilinear segments with the restriction that the first segment be linear. This approach requires that data corresponding to landing aircraft be processed in reverse time order.

Detecting Transition Points

The essential requirement for grouping a set of Cartesian coordinates into linear and curvilinear segments is the ability to detect the transition from line to

curve and from curve to line. Two methods of determining the transition point were examined. For each method, consecutive triplets of x-y coordinates are sequentially processed, beginning with the point nearest the runway. The first method, referred to as the circular method, consists of fitting a circle through the three points by finding the parameters of the equation $(x - a)^2 + (y - b)^2 = r^2$, where a and b are the x- and y-coordinates of the center of the circle. The second method, known as the triangular method, involves the construction of the perpendicular bisectors of any two sides of the triangle formed by the three points; the two bisectors intersect at the center of the circle through the three points. (See app. A.) In tests of these two methods, both gave identical results and required approximately the same amount of computer programming effort, storage, and execution time. Therefore, neither method offers any advantages over the other. The triangular method was arbitrarily chosen for all subsequent computations.

The triangular method yields a value of the radius r of the circle through the three points. When the points are collinear, r is infinite; if the points are approximately collinear, then r is large. Hence, the criterion is established that the points are considered collinear when r exceeds some value r_0; otherwise, the points define a circle of radius r. To reduce the chances of detecting a false curved segment because of random errors on x and y, the new curved segment is not considered to be legitimate unless the criterion is fulfilled at three consecutive triplets of points (i.e., five consecutive data points). The first of the five data points then defines the start of the curve.

Determining Turn Direction

Figure 3 is an illustration of the method for determining the direction of the turn (left or right). The origin of the axes is translated to the first point on the curve, then the axes are rotated such that the first two points of the curve lie on the new x-axis. The sign of the y-component of the third point in the new coordinate system determines the turn direction (positive is left, negative is right).

STATISTICAL METHODS

This section considers the techniques applied to the variables described in the previous section in order to develop the distributional properties of those variables. A brief discussion then follows on the utilization of the distributional properties in a Monte Carlo simulation to generate flight paths.

Continuous Variables

Before discussing how the best fitting distributions are found, some comments on the variables are in order. First, let Ψ_i and Ψ_{i+1} be the track angles of two line segments and θ_i the turn angle of the intervening curved segment for some pathway. Then, if θ_i is always defined to be positive, the geometry of a smooth flight path requires that $\Psi_{i+1} = \Psi_i + \theta_i$ for a right turn and $\Psi_{i+1} = \Psi_i - \theta_i$ for a left turn. In other words, if any two of these angles and the turn direction are known, then the third angle can be determined from one of these equations. In this study, the track angles are stochastically represented by best fitting distributions and turn angles calculated deterministically from the appropriate equation.

Second, the line segment lengths ℓ are positive, continuous variables bounded below by zero and (theoretically) unbounded above. Since the changes in altitude Δh are measured from the runway out along the flight path, one would expect them to be similarly bounded below by zero. As a result, the three-parameter lognormal distribution (see app. B), which is defined on the positive real axis, is considered as a possible representative distribution.

Measurements obtained with an electronic instrument such as a radar device, or the random errors associated with those measurements, are usually assumed to be normally distributed. However, it is possible that some of the variables considered here are more widely dispersed; that is, the distributions may have "fatter" tails because of pilot differences, local air turbulence, etc. Since the logistic distribution (app. B) is shaped like a normal distribution but has more area in the tails, the normal distribution and the logistic distribution are considered candidate distributions. The uniform distribution (see app. B) is the fourth continuous distribution considered since, in some small samples, the variables may appear to be uniformly distributed.

Discrete Variables

Since the altitude of an aircraft is measured in 100-ft units, initial altitude h_0 and the change in altitude Δh along any segment can be considered discrete variables. Three discrete distributions were considered as candidate representations of the change in altitude: binomial, negative binomial, and Poisson (app. B). Binomial variables are bounded below and above. The distribution itself may be symmetric or skewed in either direction and has as one characteristic a mean value which is greater than the variance. Negative binomial variables are bounded below, but unbounded above; for this distribution, the mean is less than the variance. Poisson variables are also bounded below and unbounded above, but the mean and the variance are equal. Since these distributions are defined for nonnegative integer values and since the minimum values of the initial altitude h_0 and the change in altitude Δh may be positive, the data are translated by the minimum value. The appropriate distribution to use is (app. B):

The negative binomial distribution, if $\bar{z} - z^* < s^2$

The Poisson distribution, if $\bar{z} - z^* = s^2$

The binomial distribution, if $\bar{z} - z^* > s^2$

where z^* is the minimum value and $\bar{z}$ is the mean of the random variable z. Since equality is unlikely, the Poisson distribution is chosen if $(\bar{z} - z^*)$ and the sample variance s^2 differ by no more than 5 percent. Estimation of the distribution parameters is given in appendix B. For a sample of size one, the distribution is assumed to be binomial with a zero variance.

Statistical Representations

Given samples of variables describing the air traffic on the various pathways from one runway of an airport, the procedure for determining statistical representations of the variables is relatively straightforward. For each of the variable types of a given segment, the sample mean and variance are calculated. In addition, the three-parameter lognormal statistics and the upper and lower limits of the uniform

distribution are calculated for the continuous variables. The lognormal mean and variance are found by calculating the mean and variance of the natural log of the data. The "threshold" parameter (lower bound) of this distribution is taken to be slightly smaller (about 0.1 percent) than the minimum value of the data. In reference 3, this is cited as the simplest and least accurate estimate, but it is also shown that the distribution is not sensitive to errors in the "threshold" parameter. The uniform limits are the minimum and the maximum values of the data.

Fitting Distributions

Selection of the best fitting continuous distribution to a set of segment variables is made by applying the Kolmogorov-Smirnov one-sample test (ref. 4) to the variables on each segment and to each of the four continuous distributions. The Kolmogorov-Smirnov test provides a nonparametric statistical measure of the deviation between a hypothesized distribution and the sample distribution of the segment variable. The significance level is defined to be the probability of rejecting a distribution when the data actually are a sample from that distribution. The best fitting continuous distribution is the one with the minimum significance level based on the Kolmogorov-Smirnov statistic. For the initial altitude and change in altitude, the appropriate discrete distribution is chosen according to the relationship between the mean and the variance.

Probabilities of Alternative Paths

As indicated in figure 2, an aircraft can follow three or more alternative paths at points A, B, and C. Based on the original data, the ground track at point A, for example, is modeled as a line segment (L1), a left turn (C1, if $\theta > 90°$; C2, if $\theta < 90°$), or a right turn (C5, if $\theta < 90°$; C8, if $\theta > 90°$). By counting the aircraft on each segment, the probability of an aircraft using a particular alternative path is readily calculated as the ratio of the number using the alternative path to the number using the previous segment.

Once the best fitting distributions of the variables and the path probabilities have been determined, the air traffic for a given runway has been statistically modeled. Although it was not a part of this study, it is also easy to stochastically model total traffic for an airport by determining the probable use of each runway.

MONTE CARLO SIMULATION METHOD

All of the random numbers required for simulating the flight paths can be calculated from standard normal and uniform random variables generated by standard techniques (ref. 5). Random variables of specific normal and uniform distributions are obtained by appropriate translation and scaling of the respective standard variables. Lognormal variables are calculated by logarithmic transformation of standard normal variables. Logistic and discrete random variables are obtained by applying the appropriate inverse cumulative distribution function to standard uniform random variables.

Given a statistical model of flight paths on each runway, a Monte Carlo simulation can be readily performed. Let N be the number of flight paths to be generated for one runway. For each flight path, the initial coordinates (x_0, y_0, h_0) and the

variables of the first line segment are randomly generated; Cartesian coordinates of points along this segment are generated. (See app. A.) A uniformly generated random number is compared to the unit interval which has been subdivided according to the path probabilities in order to determine the next segment to be generated at points A, B, and C. The general procedure is to randomly select a path when necessary, generate random variables appropriate to the distributions of the current segment, and generate coordinates of points on that segment before moving to the next segment of the flight path. This procedure is repeated N times for the desired N flight paths.

APPLICATION TO DULLES AIRPORT DATA

This section presents the application of the preceding analysis and simulation procedures to flight-track data supplied by the Federal Aviation Administration (FAA) for flights at Dulles International Airport as an illustrative example. All of the calculations required for these procedures were performed on Control Data CYBER 170 series computers at NASA Langley Research Center.

Description of Dulles Data

Shown in figure 4 are the runway configuration, the runway numbering scheme, and the relative location of the radar at Dulles International Airport. The system coordinate origin is the Dulles terminal radar located at 38°57'24" North; 77°27'50" West. The raw FAA data consist of aircraft type identifier, unique track identifier, flight number, time tags, and Cartesian coordinates of 678 flight operations at Dulles on July 24 and July 30, 1979. The x-y coordinates are measured in units of 256ths of a nautical mile (1 n.mi./256 = 23.75 ft) from the radar, and the altitude is given in hundreds of feet. All data points were coarsely smoothed by the FAA using a three-point moving average.

All of the general-aviation, nonscheduled-commercial, and military flights were discarded from the data set in order to focus on the trajectories of commercial jet transports. The ground tracks of the remaining arrivals and departures are illustrated in figures 5 and 6; these plots include data points corresponding to aircraft taxiing on the ground. These latter points were eliminated from the analysis by using a minimum altitude of 500 ft. Some of the illustrated ground tracks were also eliminated because they represented aircraft passing through the area, practicing landings, or incomplete data-point sets. For example, the loop south of runway 5 in figure 5 represents an aircraft performing a "touch and go" prior to the actual landing.

Modifications for Dulles Data

The set of flight paths selected for use in this study consists of 135 arrivals and 105 departures on runways 1 to 5. Table I is a list of the number of flights by runway. Throughout the study, arrivals and departures are considered separately since the characteristics of the two types of flight paths differ. For a departing flight, the initial linear segment (L2) is quite straight and is usually shorter than the same segment for an arriving flight. The differences in length and linearity of this segment for the two types of flights are a result of the navigational freedom of a departing aircraft to turn soon after leaving the runway and the requirement of an arriving aircraft to align its path with the runway. For many arriving flights, the

initial linear segment contained several shallow turns indicating possible overcompensation for crosswinds and other turbulence. In order to reduce the effect of the shallow turns when determining the transition to a "true" curvilinear segment, the x-y coordinates of only the arrival data were additionally smoothed with a five-point moving average.

A value of 2.5 n.mi. was used for the threshold radius r_0 to distinguish between linear and curvilinear segments. The choice of r_0 is critical since a small value will cause points on wide turns to be treated as lines, and a large value will cause noisy points on a line to be treated as turns. The latter situation may be a result of atmospheric turbulence or shallow maneuvers during a landing approach. The value of 2.5 n.mi. was determined experimentally from the Dulles data and is acceptable based on a visual comparison of the data and the fitted segments.

Treatment of Track-Angle Anomalies

With the exception of the track angle Ψ, the segment variables are well-defined by the radar data. The track angles for north-heading linear segments present a special problem, particularly for the initial segments from runways 2 and 4. For aircraft flying west of north, the track angle is near 360°, and for aircraft flying east of north, the track angle is close to 0°; the mean of all such northbound track angles is, therefore, about 180° (south). This error can be corrected by adding 360° to the east-of-north track angles before calculating any statistics.

Particular attention was required for the one difficulty that arose in generating track angles from the distributions. Because of small sample sizes and large dispersions, the track-angle distributions for successive linear segments (for example, L5 and L6 in fig. 2) sometimes intersected. The result was a loop in the simulated ground track. For example, the path from L5 to L6 requires a left turn through C3, with the track angle on L6 being less than that on L5. When the distributions intersect (see sketch), it is possible to generate a track angle on L6

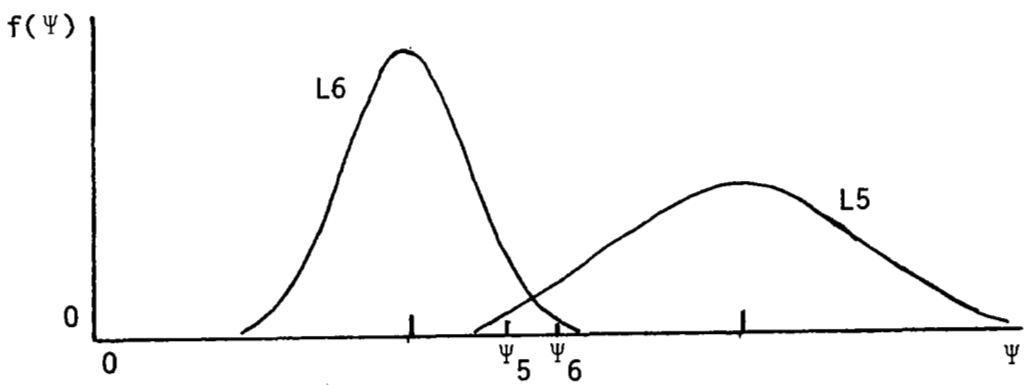

greater than the track angle on L5 which would suggest a right turn; however, the model specifies C3 as a left turn and a left turn of almost 360° to the new track angle on L6 results. In order to virtually eliminate intersecting distributions for this variable, the standard deviations of the two intersecting distributions were adjusted down and both distributions were thereafter assumed to be normal. The standard deviations were adjusted so that the midpoint between the two means is at

least 3.2 standard deviations from each mean. This reduces the chances of the two distributions intersecting by a factor of 100.

Distributions of Continuous Variables

The number of best fitting distributions found for the continuous variables are shown in table II. Each best fit distribution results from applying the Kolmogorov-Smirnov test to the possible distributions that may fit all measurements of one variable (such as r) on one segment. Table II does not include results for samples of size one or two for which the distributions are assumed to be normal; for a sample of size one, the variance is taken to be zero (i.e., the variable is deterministic). Comparison of the best fitting distributions for various sample sizes indicated that there was a slight correspondence between sample size and type of distribution which best fits a sample. For the initial ground-track coordinates (x_0, y_0), the type of distribution appears to be independent of sample size. The numbers in parentheses in table II indicate the number of best fitting distributions for which the significance level in the Kolmogorov-Smirnov test is less than 0.1.

For the distance variables (ℓ and r), the normal was the best fitting distribution for sample sizes ranging from 3 to 45. The logistic distribution was best fitting for sample sizes from 4 to 29, and the lognormal distribution was best fitting for sample sizes from 3 to 33. However, the best fitting normal and logistic distributions occurred fairly uniformly over all the sample sizes; whereas, 10 out of 13 lognormal distributions best fit samples of size 10 or less. The lognormal distribution tends to fit smaller samples, apparently because a small sample is more easily skewed by one or two random values than a large sample. The uniform distribution best fits only one sample of size 6; this evidently is the result of a small sample appearing uniformly distributed by chance. In general, the continuous variables appear to be fit best by distributions which are symmetric and unimodal (normal or logistic).

Distributions of Discrete Variables

Presented in table III are the results of fitting discrete distributions to the altitude data (initial altitude h_0 and change in altitude along a segment Δh). The table does not include binomial distributions resulting from samples of size 1. Prior to comparing the mean and the variance in order to select the appropriate distribution, the initial altitude was shifted to the origin by h^* and the change in altitude by the minimum Δh value for each segment. As indicated in table III, these two types of variables are overwhelmingly best represented by negative binomial distributions. The initial altitudes in the arrival data best described by a Poisson distribution occurred on runway 4 where all 12 initial altitudes were equal to the minimum value of 500 ft. The binomial and Poisson representations resulted in sets of size 11 and 3, respectively, and may be chance occurrences. Generally, the variances of these data exceed the respective means because h_0 and Δh have fixed lower limits and somewhat restricted upper limits. The upper limits result from ascent/descent rates constrained by aircraft capabilities and passenger comfort. The net result is that the negative binomial distribution generally provides the best representation of the altitude variables. It is interesting to note that all initial altitudes in the arrival data (that is, altitudes at the point closest to the runway end) were less than 1100 ft; in the departure data, only 60 percent of the

initial altitudes were less than 1100 ft. This difference is indicative of the pilots' attempts to land smoothly along shallow slopes and to gain altitude rapidly during takeoffs.

Test of Simulation Model

To test the simulation model, 50 flights each of arrivals and departures per runway on runways 1 to 5 were generated using the best fitting distributions from the arrival and departure data analyses. Arrival paths on runway 1 and departure paths on runway 4 were not generated because of the small number of flights on those runways in the original data. The ground tracks from the simulations are shown in figures 7 and 8. Comparison of figures 5 and 6 with figures 7 and 8 indicates the accuracy of the simulation model. However, three thoughts must be kept in mind when examining these figures: (1) some of the ground tracks shown in figures 5 and 6 were eliminated from the analysis, (2) the simulation results are based on only a five-segment flight-path model, and (3) the number of flights per runway in the original data is generally less than 50. In general, the model simulates the actual flight paths very well.

As a further comparison of the simulated data with the Dulles data, plots of altitude with respect to x- and y-coordinates are presented in figures 9 to 12 for the original and the simulated data. Comparisons of actual and simulated data are illustrated in figures 9 and 10 for arrival data on runway 3 and in figures 11 and 12 for departure data on runway 5. These runways were chosen for comparison because they bore the heaviest traffic in the original data. The figures indicate that the simulated flight paths follow the same general trends as the actual flight paths. The most visible weakness of the simulation model appears to be the larger dispersions of the simulated flight paths. The larger dispersions are apparently because of large estimated variances of segment variables which could be caused by the small samples available. Small samples can be expected on segments 4 and 5 of any pathway unless the pathway bears a large proportion of the traffic or the corresponding runway is frequently used.

CONCLUDING REMARKS

In the analysis discussed here, the radar tracking coordinates of points along an aircraft flight path have been used to reconstruct the flight path as an alternating sequence of joined linear and curvilinear segments in three-dimensional space. Each of the segments is completely described by three variables and, for curvilinear segments, a turn direction. The basic linear and curvilinear segments were combined to produce a nine-path model of air traffic applicable to any runway. Several of these runway traffic models can then be combined to model the air traffic at any airport.

The model discussed was applied to radar tracking data of commercial flights at Dulles International Airport. The continuous segment variables (length, radius, and initial position) derived from the Dulles data were generally found to be best represented as normal or normal-like probability distributions. The discrete altitude variables (initial altitude and change in altitude along a segment) were best described by negative binomial distributions. A Monte Carlo simulation of Dulles arrival and departure flight paths based on the derived probability distributions

compared very favorably with the original data. The techniques presented in this paper, therefore, provide reasonable approaches to modeling and simulating near-terminal aircraft flight paths.

Langley Research Center
National Aeronautics and Space Administration
Hampton, VA 23665
March 4, 1982

TABLE I.- NUMBER OF USABLE COMMERCIAL FLIGHTS IN DULLES DATA SET

Runway	Arrivals	Departures
1	1	21
2	19	17
3	54	24
4	12	3
5	49	40
6	0	0
Total	135	105

TABLE II.- NUMBER OF BEST FITTING DISTRIBUTIONS FOR CONTINUOUS VARIABLES

Variable	Probability distribution[a]			
	Normal	Lognormal	Logistic	Uniform
Arrivals				
x_0	1(0)	2(0)	1(0)	0
y_0	2(1)	2(0)	0	0
ℓ	12(6)	4(2)	1(1)	0
r	4(4)	4(4)	1(1)	0
Departures				
x_0	1(1)	2(2)	2(0)	0
y_0	3(1)	1(1)	1(0)	0
ℓ	10(4)	3(1)	3(1)	1(1)
r	5(5)	2(2)	2(1)	0

[a]Numbers in parentheses show number of distributions with significance level less than 0.1.

TABLE III.- NUMBER OF BEST FITTING DISTRIBUTIONS FOR DISCRETE VARIABLES

Variable	Probability distribution		
	Binomial	Negative binomial	Poisson
Arrivals			
h_0	0	3	1
Δh (line)	1	16	0
Δh (curve)	0	8	1
Departures			
h_0	0	5	0
Δh (line)	0	17	0
Δh (curve)	0	9	0

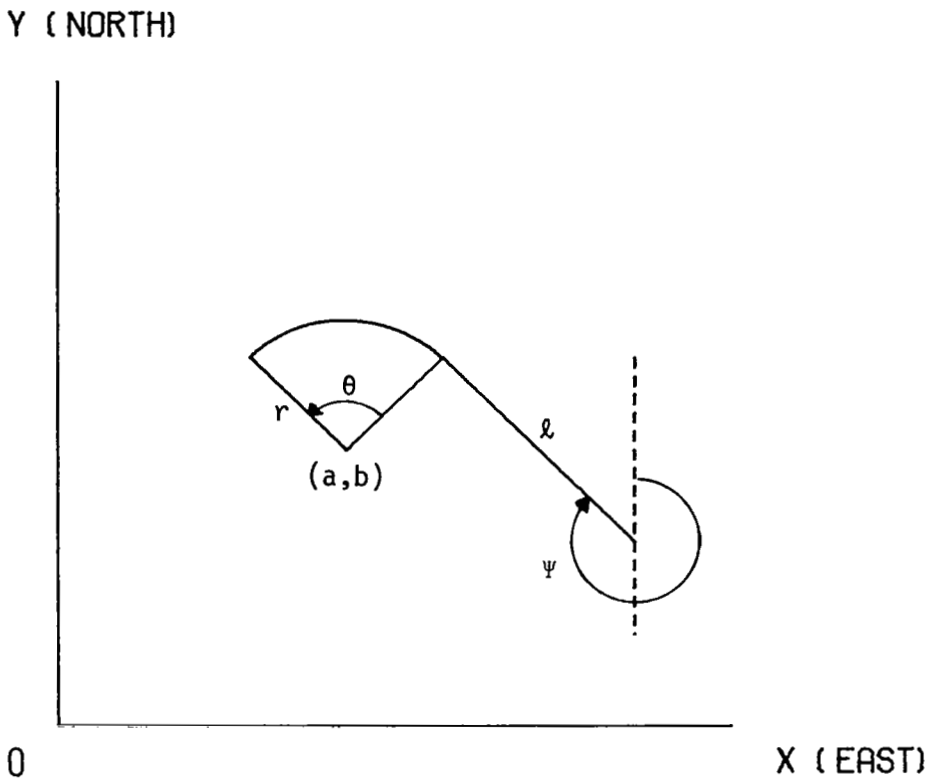

Figure 1.- Variables used to describe ground track of two segment types.

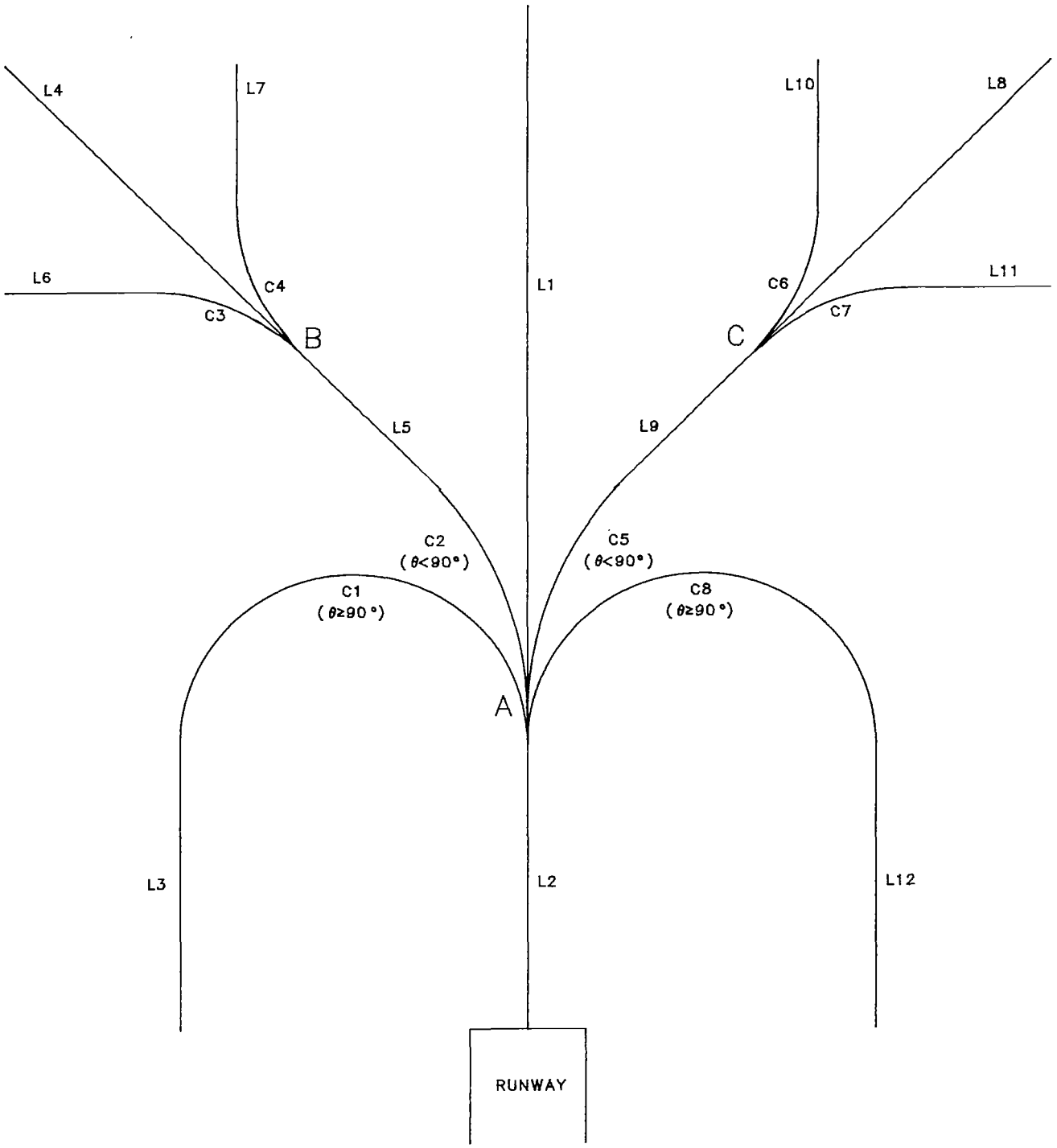

Figure 2.- Possible flight paths emanating from runway.

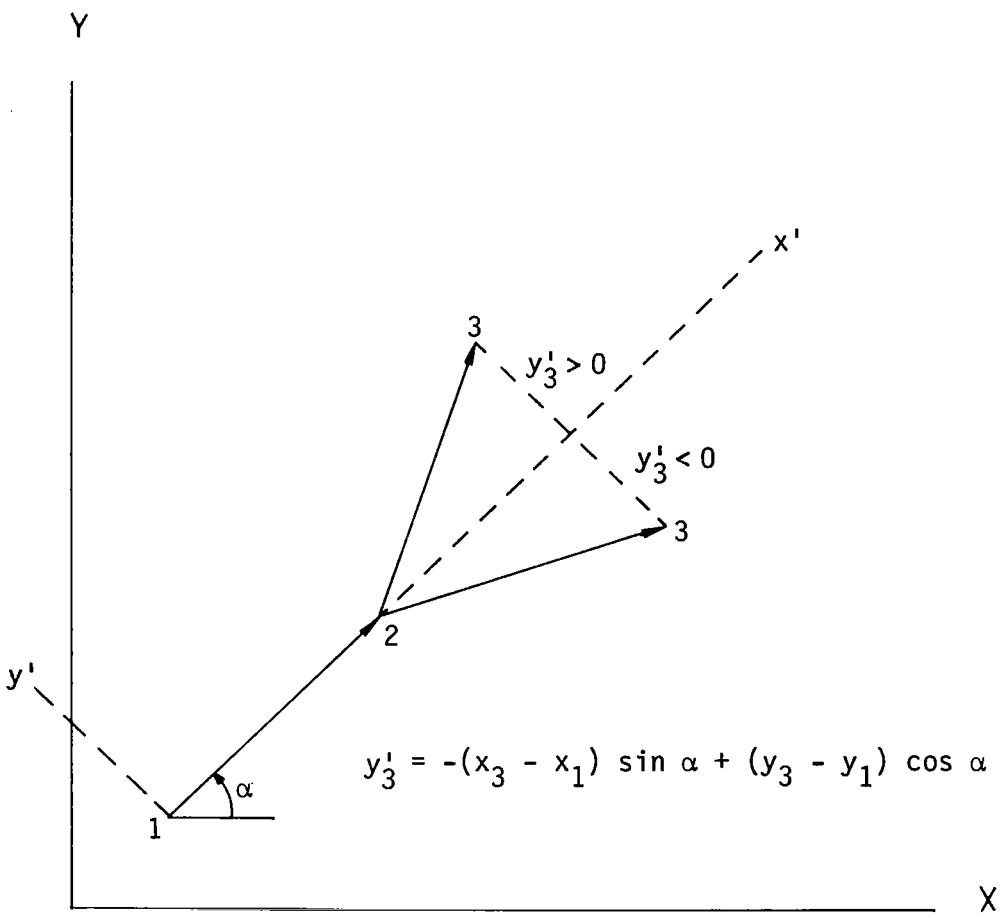

Figure 3.- Discrimination between left and right turns.

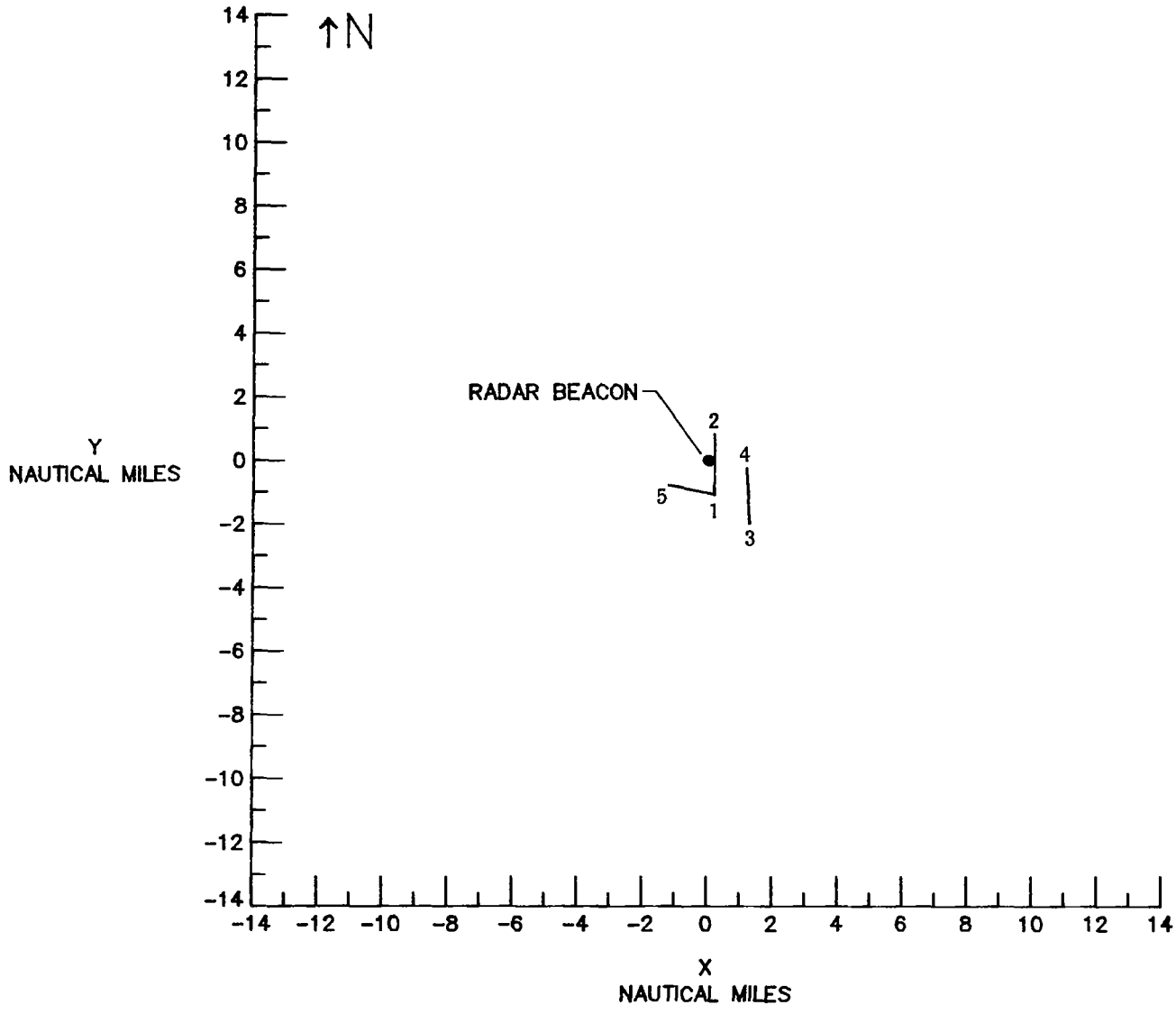

Figure 4.- Orientation of runways and radar at Dulles International Airport.

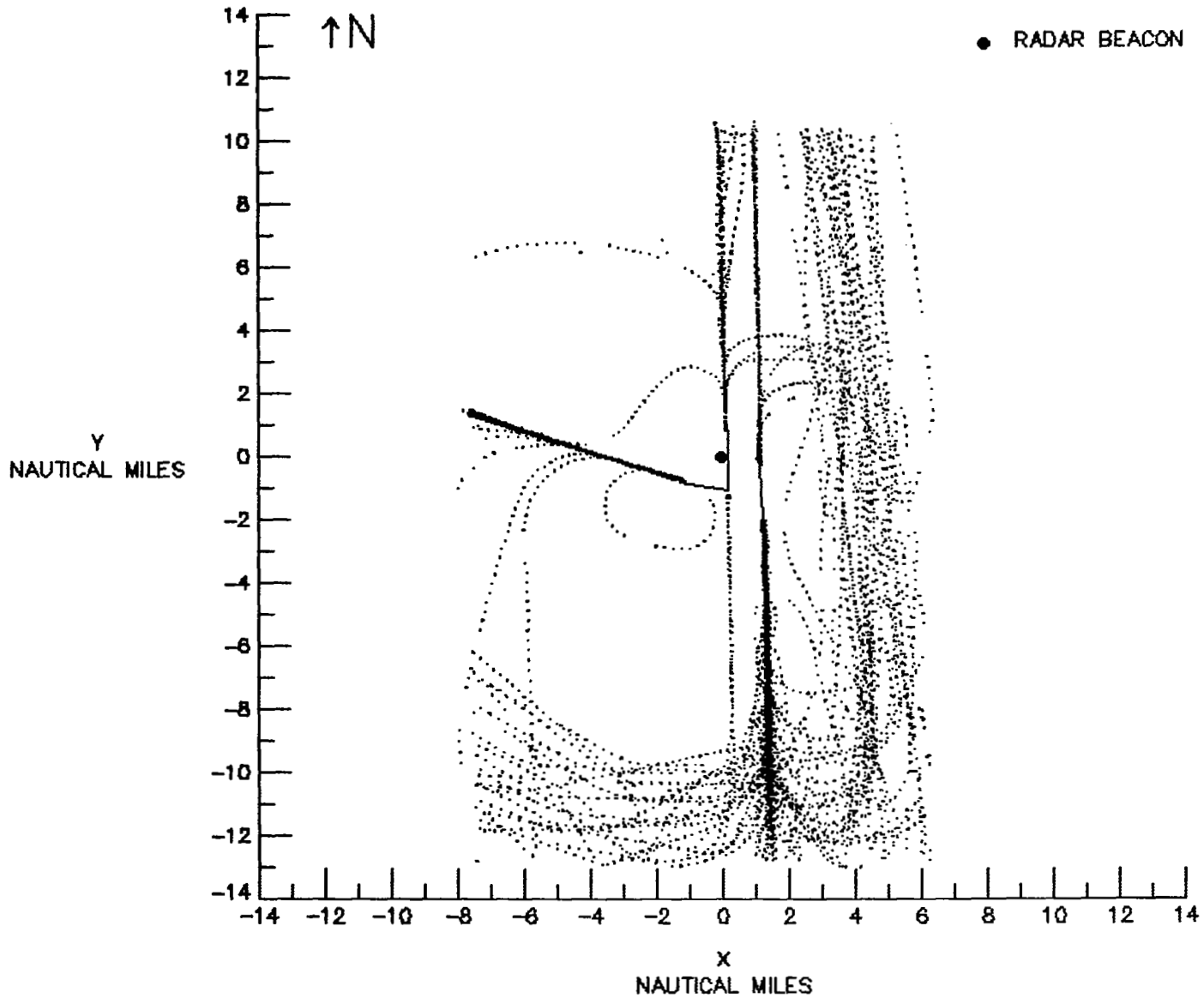

Figure 5.- Ground tracks of actual arrivals at Dulles International Airport.

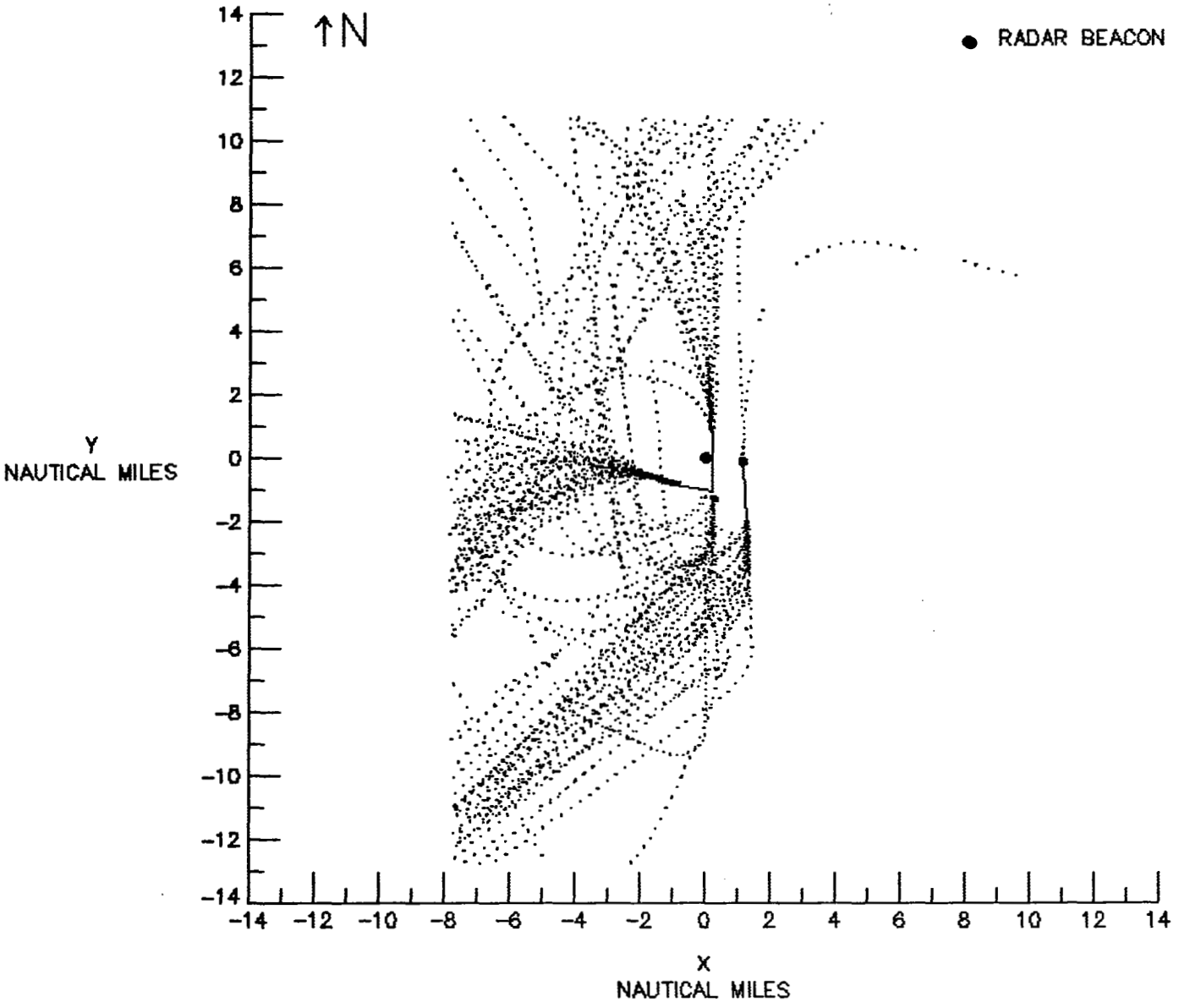

Figure 6.- Ground tracks of actual departures at Dulles International Airport.

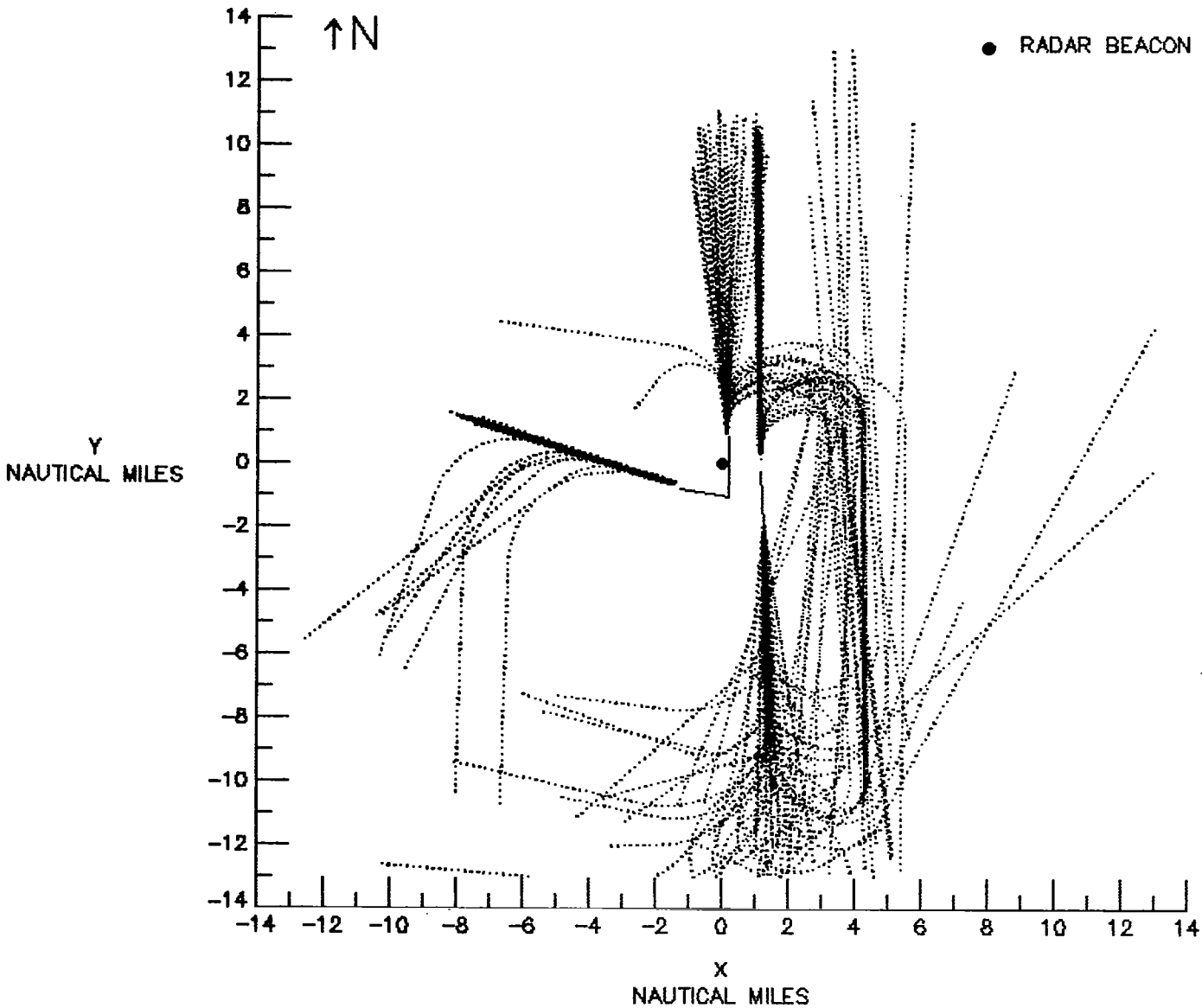

Figure 7.- Ground tracks of simulated arrivals at Dulles International Airport.

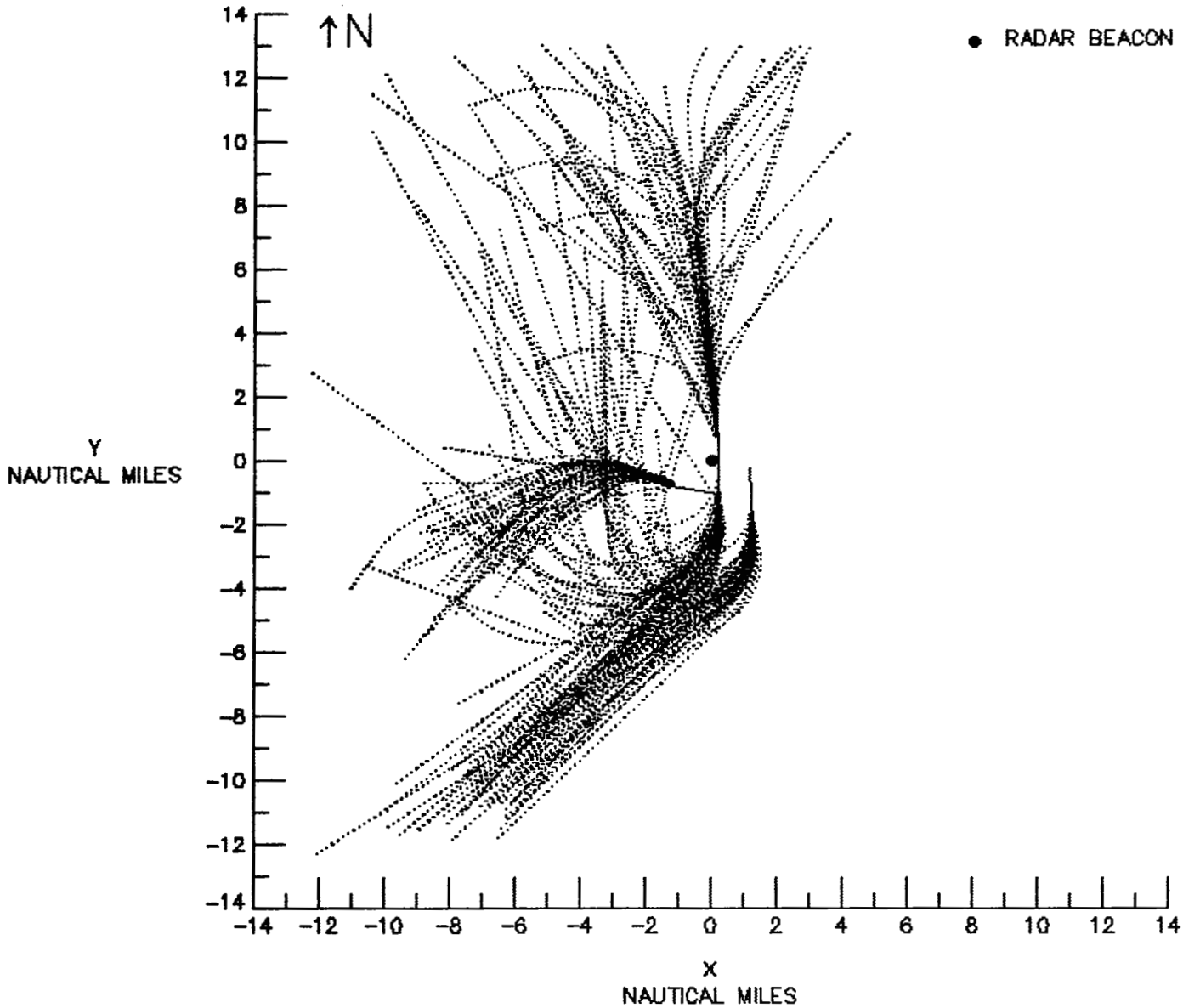

Figure 8.- Ground tracks of simulated departures at Dulles International Airport.

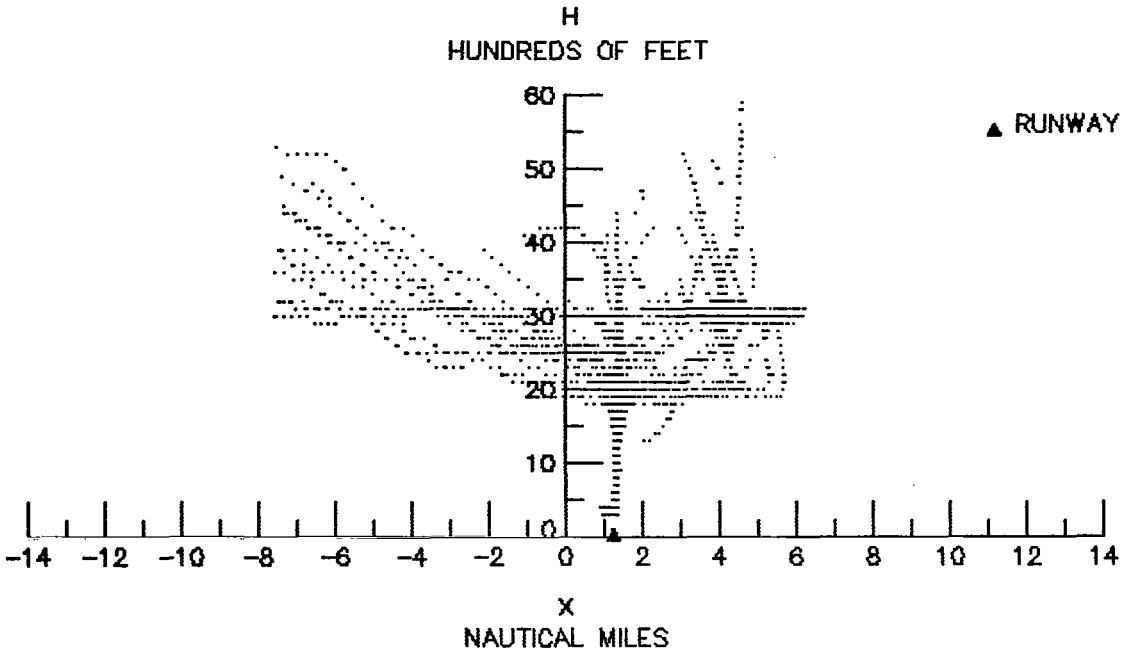

(a) Actual.

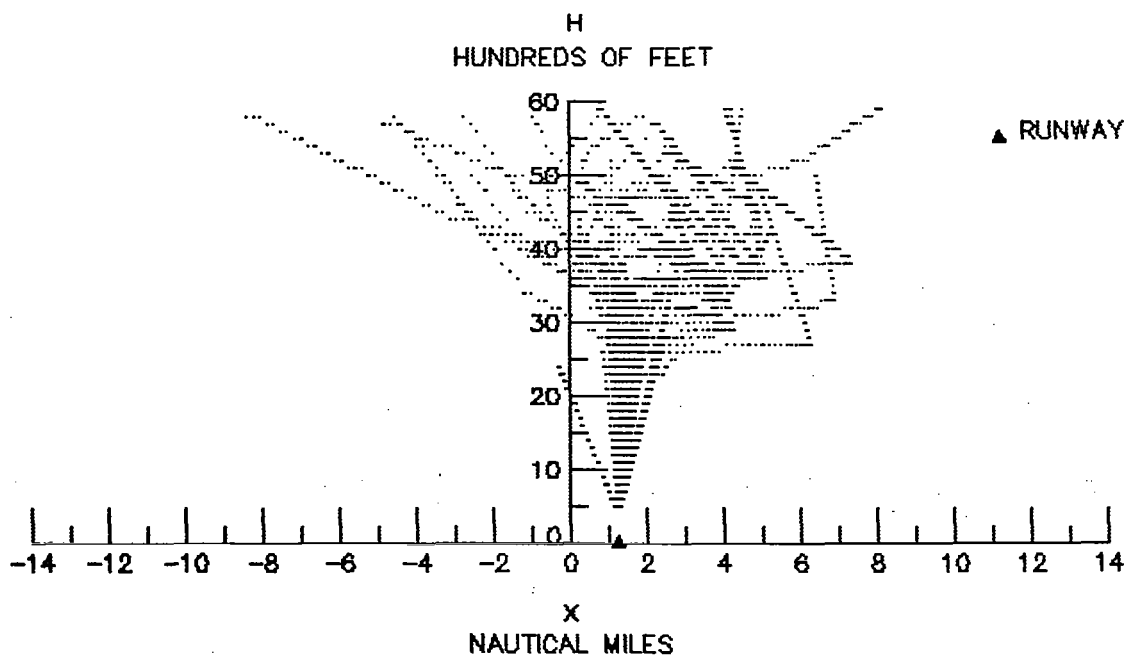

(b) Simulated.

Figure 9.- Altitude of arrivals on runway 3 at positions east (+) and west (-) of radar beacon at Dulles International Airport.

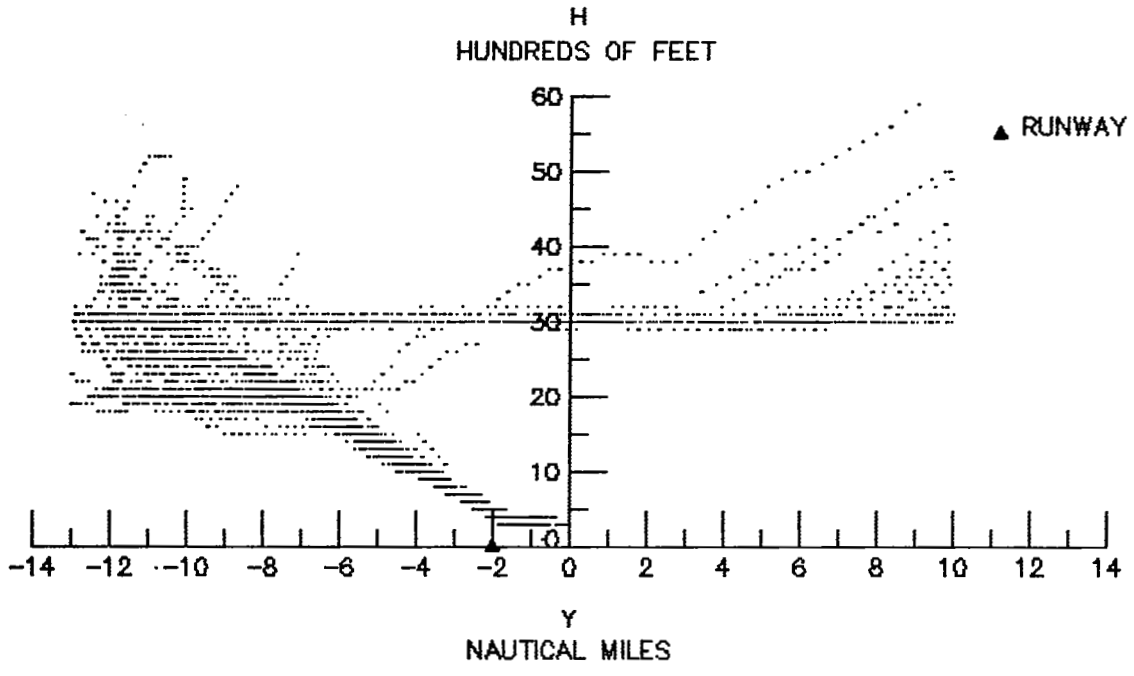

(a) Actual.

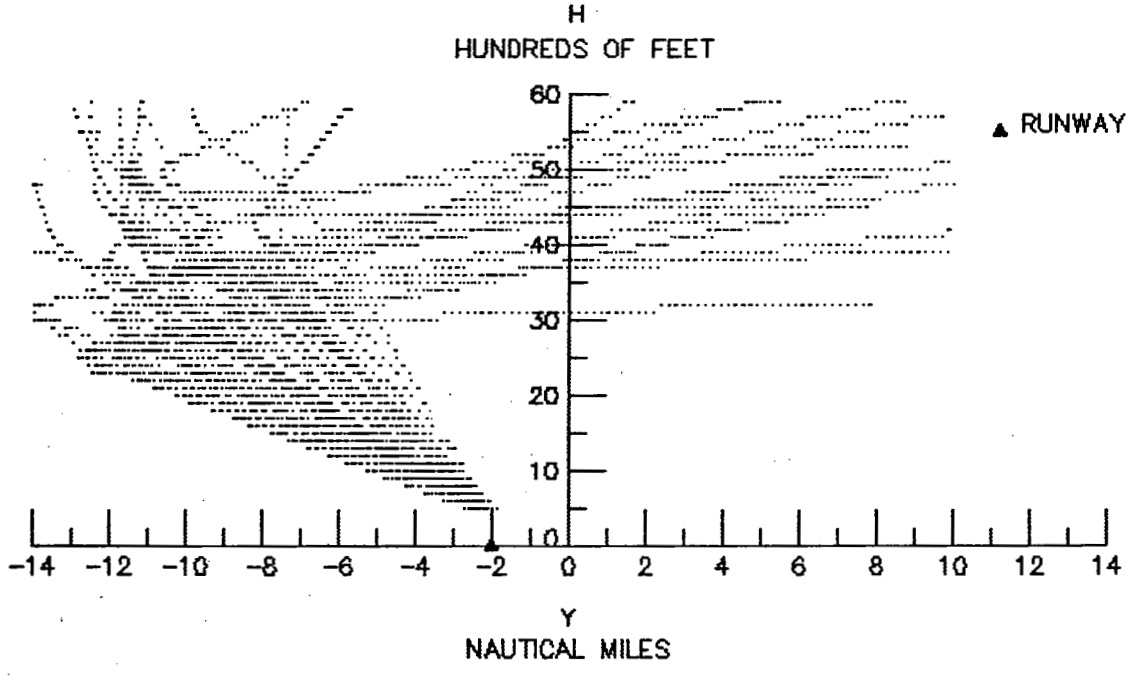

(b) Simulated.

Figure 10.- Altitude of arrivals on runway 3 at positions north (+) and south (-) of radar beacon at Dulles International Airport.

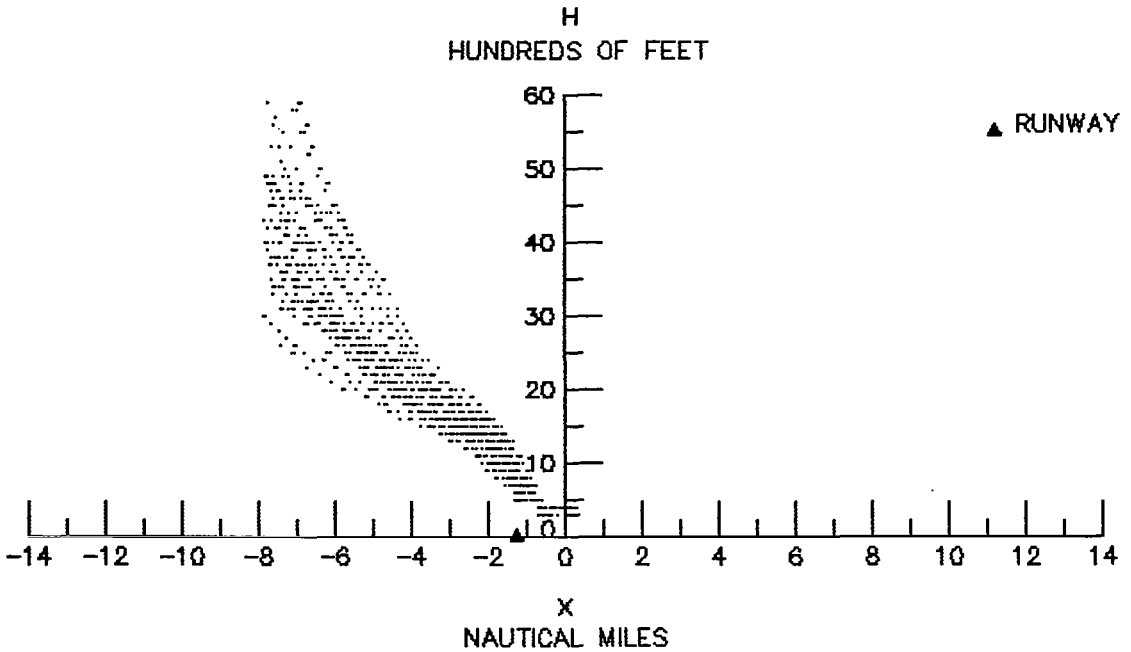

(a) Actual.

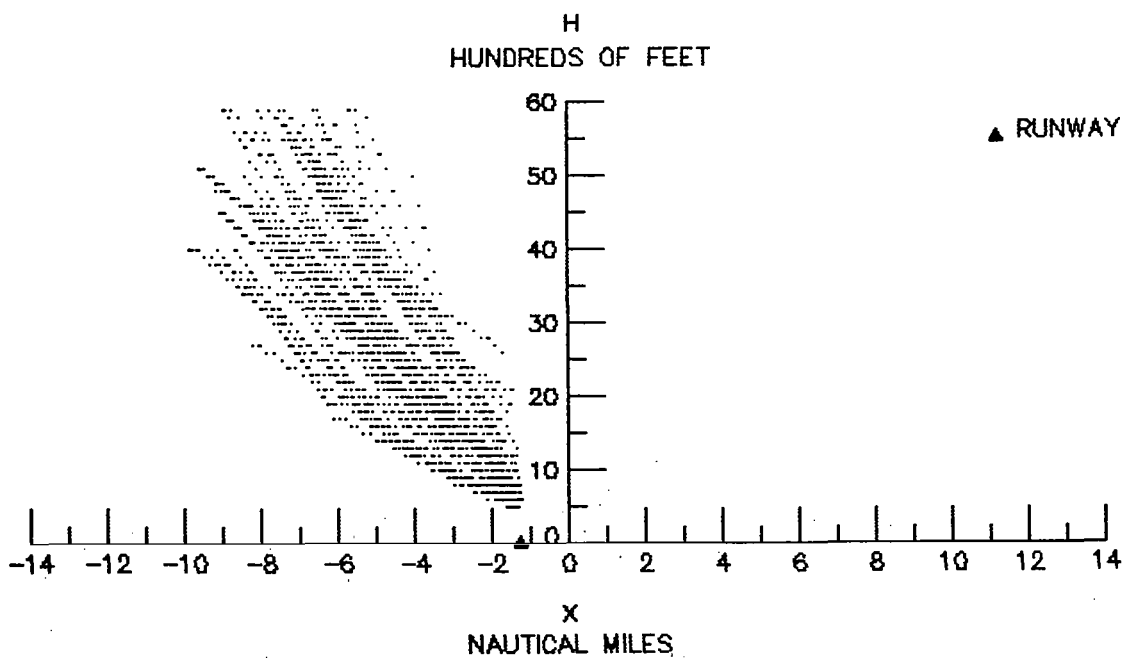

(b) Simulated.

Figure 11.- Altitude of departures on runway 5 at positions east (+) and west (-) of radar beacon at Dulles International Airport.

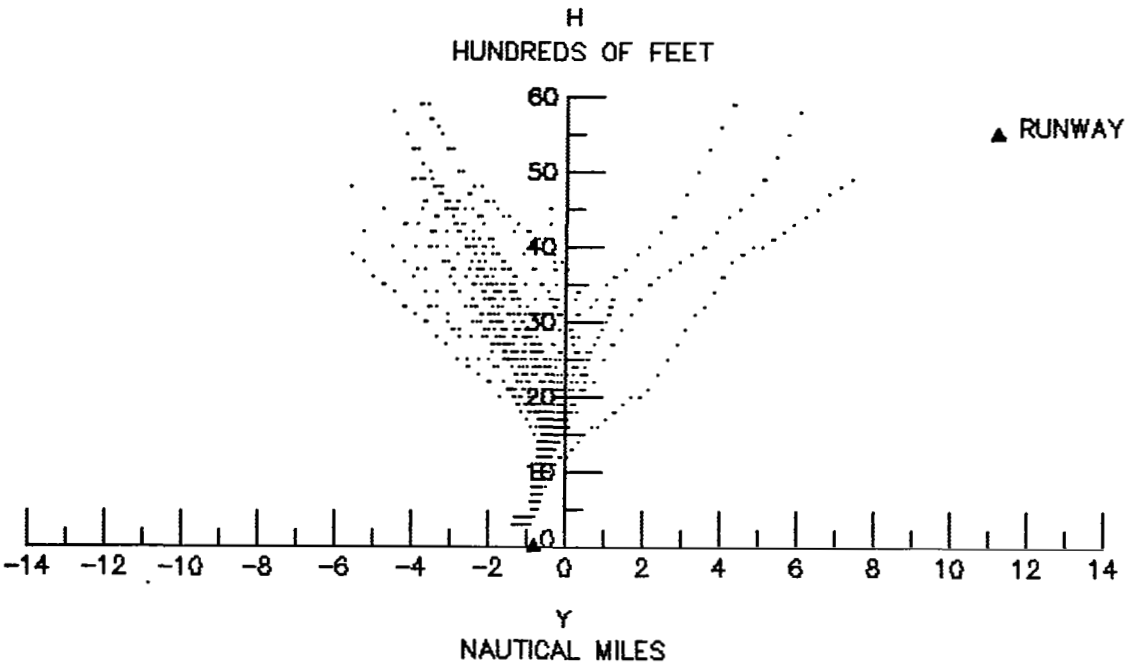

(a) Actual.

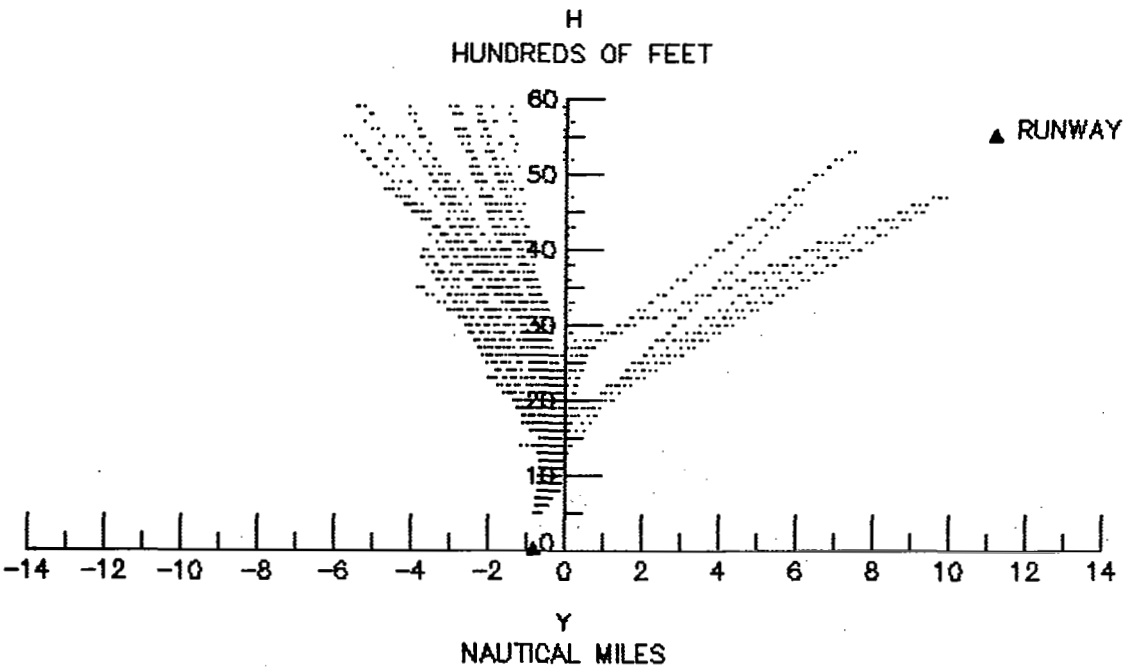

(b) Simulated.

Figure 12.- Altitude of departures on runway 5 at positions north (+) and south (-) of radar beacon at Dulles International Airport.

APPENDIX A

ANALYTIC GEOMETRY OF FLIGHT PATHS

Triangular Method of Fitting a Circle

Let (x_1,y_1), (x_2,y_2), and (x_3,y_3) be the Cartesian coordinates of three points in two-dimensional space. Without loss of generality, consider the line segments between (x_1,y_1) and (x_2,y_2) and between (x_2,y_2) and (x_3,y_3). Points along the perpendicular bisector of either line segment are equidistant from the two points defining the segment. The intersection of the two perpendicular bisectors is, therefore, equidistant from all three points and defines the center of the circle through the points. If the perpendicular bisectors do not intersect, then essentially the points lie on a circle of infinite radius; this is equivalent to the three points being collinear.

Consider first the points (x_1,y_1) and (x_2,y_2). The line segment from the first point to the second point has slope $(y_2 - y_1)/(x_2 - x_1)$ and is given by the equation $y = y_1 + (x - x_1)(y_2 - y_1)/(x_2 - x_1)$. The point of bisection of this line segment is at $(0.5(x_1 + x_2),\ 0.5(y_1 + y_2))$. For a line perpendicular to this line, the slope is the negative reciprocal of the original slope, or $-(x_2 - x_1)/(y_2 - y_1)$. Therefore, the equation of a line through the point of bisection and perpendicular to the line segment from (x_1,y_1) to (x_2,y_2) is:

$$y = 0.5(y_1 + y_2) - [x - 0.5(x_1 + x_2)](x_2 - x_1)/(y_2 - y_1) \qquad \text{(A1)}$$

By a similar argument, the equation of the perpendicular bisector of the line segment from (x_2,y_2) to (x_3,y_3) is:

$$y = 0.5(y_2 + y_3) - [x - 0.5(x_2 + x_3)](x_3 - x_2)/(y_3 - y_2) \qquad \text{(A2)}$$

The center of the circle is the simultaneous solution of equations (A1) and (A2).

Generating Points Along Segments

Let the initial point (x_i,y_i,h_i), altitude change (Δh), length (ℓ), and track angle (Ψ) of a line segment be given. In order to generate points spaced $\Delta\ell$ units apart along the segment, let $m = \ell/\Delta\ell$ be the number of points to be generated. The coordinates of the points are given by

$$x_j = x_i + j\ \Delta\ell \sin \Psi$$

$$y_j = y_i + j\ \Delta\ell \cos \Psi$$

$$h_j = h_i + j\ \Delta h/m$$

where $j = 1,2,\ldots,m$.

APPENDIX A

For curved segments beginning at (x_i, y_i, h_i) and having radius (r), turn angle (θ), and altitude change (Δh), the previous line segment must be tangent to the arc at the initial point of the arc. Let Ψ be the track angle of the previous line segment, $\Delta\ell$ be the spacing of the points along the arc, $m = r\theta/\Delta\ell$, and $\Delta\theta = \theta/m$. Let turn direction be indicated by $T = +1$ for a left turn, $T = -1$ for a right turn. The coordinates of the points along the curve are given by the equations

$$\beta_j = (\pi - j\ \Delta\theta)/2$$

$$R_j = 2r \cos \beta_j$$

$$x_j = x_i + R_j \sin (\Psi - Tj\ \Delta\theta/2)$$

$$y_j = y_i + R_j \cos (\Psi - Tj\ \Delta\theta/2)$$

$$h_j = h_i + j\ \Delta h/m$$

where $j = 1, 2, \ldots, m$.

These equations are easily derived from sketch A1.

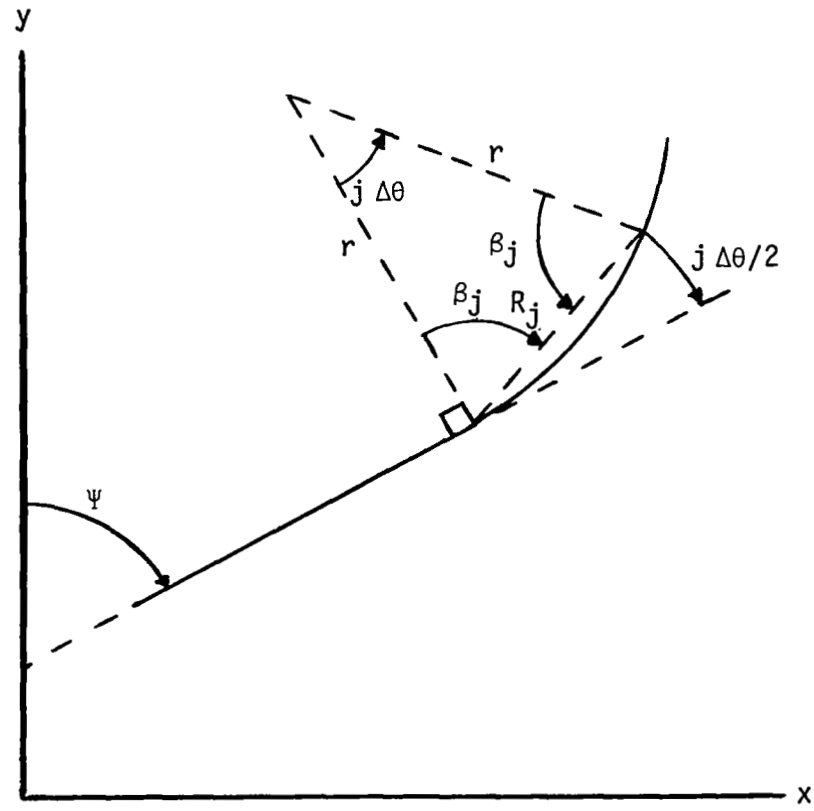

Sketch A1

APPENDIX B

PROBABILITY DISTRIBUTIONS

This appendix briefly describes the probability distributions used in this study. For each distribution, the presentation includes the probability density function (pdf) defining the distribution and includes the equations used to estimate the parameters of the distribution.

Continuous Distributions

The pdf of a continuous random variable must fulfill two conditions. The first condition is that the pdf (f(z)) is nonnegative for all real values of z. Second, the integral of f(z) over all z is equal to 1 (ref. 3).

Uniform distribution.- The uniform distribution (ref. 6) has the pdf

$$f(z) = \begin{cases} \dfrac{1}{e - d} & (d \leq z \leq e) \\ 0 & (\text{Otherwise}) \end{cases}$$

This pdf defines the distribution of what are commonly called random numbers. Since d and e define the limits of the interval over which f(z) is positive, they may be estimated from a random sample by setting d equal to the minimum of the sample and e equal to the maximum. The distribution is illustrated in sketch B1.

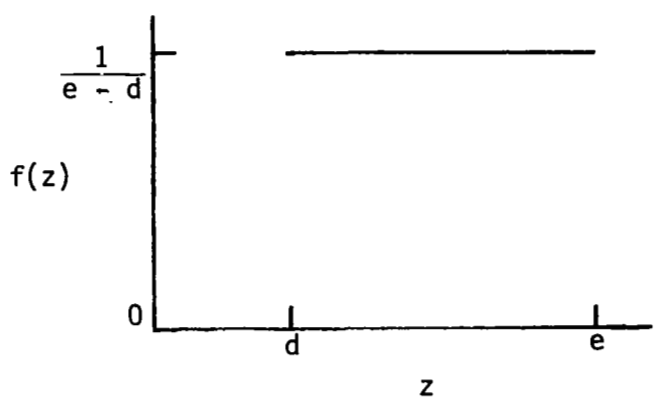

Sketch B1

APPENDIX B

Normal distribution.- This is the symmetric, bell-shaped, or Gaussian distribution (ref. 3) usually associated with instrumentation errors or "noise." The pdf is

$$f(z) = \frac{1}{\sigma\sqrt{2\pi}} \exp\left\{\frac{-(z - \mu)^2}{2\sigma^2}\right\} \qquad (-\infty < z < \infty)$$

The parameters μ and σ are the population mean and the standard deviation which are directly estimated by the sample mean $\bar{z}$ and the standard deviation s. The distribution is shown in sketch B2.

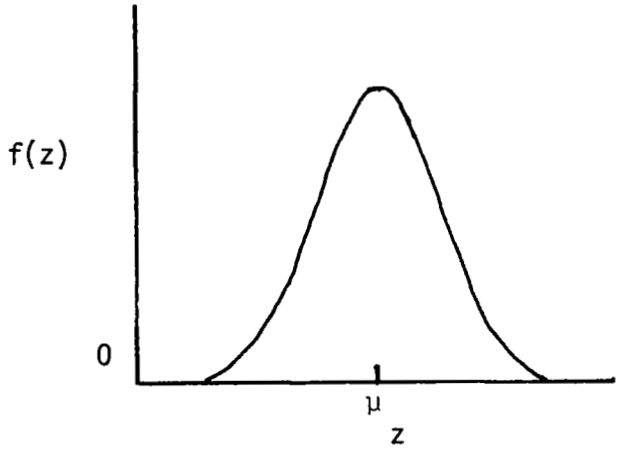

Sketch B2

Logistic distribution.- The logistic distribution (ref. 6) shown in sketch B3 is shaped very much like a normal distribution (see sketch B2) except it has a larger

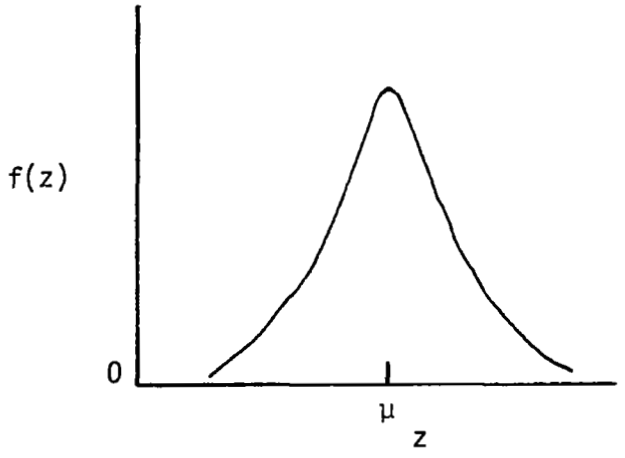

Sketch B3

kurtosis (peakedness) and correspondingly more probability in the tails. The logistic pdf is

$$f(z) = \frac{\pi}{\sigma\sqrt{3}}[\exp\{-\pi(z - \mu)/(\sigma\sqrt{3})\}]/[1 + \exp\{-\pi(z - \mu)/(\sigma\sqrt{3})\}]^2$$

for $-\infty < z < \infty$. The parameters μ and σ are the population mean and the standard deviation and are estimated by $\bar{z}$ and s. This distribution can be derived in several ways, such as the solution of an ordinary differential equation describing growth curves.

Lognormal distribution.- The three-parameter lognormal distribution (sketch B4) is defined by the probability density function (ref. 3),

$$f(z) = \begin{cases} [(z - \tau)\sigma\sqrt{2\pi}]^{-1} \exp[-0.5\{\log (z - \tau) - \mu\}^2/\sigma^2] & (z > \tau) \\ 0 & (\text{Otherwise}) \end{cases}$$

In this function, τ is the threshold parameter and μ and σ are the mean and the standard deviation of $\log (z - \tau)$. The name is derived from the fact that if z has a lognormal distribution then $\log (z - \tau)$ is normally distributed. This is illustrated by substituting $\log (z - \tau)$ for z in the normal pdf. The lognormal distribution has proven useful in describing the distribution of particle sizes and of critical drug dosages. The distribution is skewed to the right (see sketch B4) with the majority of the probabilities associated with values less than the mean.

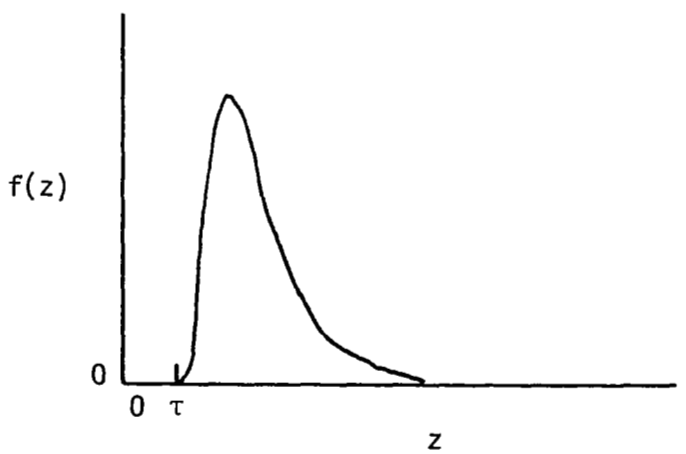

Sketch B4

From a random sample of data, the threshold τ can be estimated using a value less than or equal to the minimum of the sample. The mean and standard deviation (μ and σ) are estimated by transforming the sample with $z' = \log (z - \tau)$ and calculating the sample mean and the standard deviation of z'.

APPENDIX B

Discrete Distributions

Discrete distributions describe the probability of discrete events occurring and are therefore defined on the (usually nonnegative) integers. A discrete probability density function must be nonnegative for all integer values and must sum to one over all the integers (ref. 7).

Binomial distribution.- This distribution describes the probability of obtaining z successes in n independent trials when the probability of success on one trial is $p(0 \leq p \leq 1)$. A common experiment to which this distribution applies is the tossing of a coin n times. The probability density function (ref. 7) is given by

$$f(z) = \begin{cases} \binom{n}{z} p^z (1 - p)^{n-z} & (z = 0, 1, 2, \ldots, n) \\ 0 & (\text{Otherwise}) \end{cases}$$

This distribution may be symmetric or skewed to the left or right. As shown in sketch B5, the distribution skewed slightly to the right.

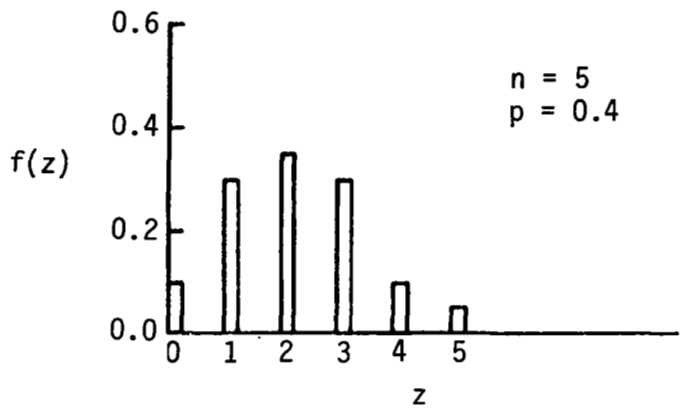

Sketch B5

Since the mean and variance are np and $np(1 - p)$, respectively, n and p are estimated from $\bar{z}$ and s^2 by

$$n = \bar{z}^2/(\bar{z} - s^2)$$

and

$$p = 1 - (s^2/\bar{z})$$

Note that estimation of positive n and p requires $\bar{z} > s^2$.

APPENDIX B

Negative binomial distribution.- This distribution is complementary to the binomial distribution in the sense that it provides the probability for needing to perform z number of independent trials in order to obtain M successes when the probability of success on each trial is p. In terms of this definition, the pdf (ref. 7) is given by

$$f(z) = \begin{cases} \binom{z-1}{M-1} p^M (1-p)^{z-M} & (z = M, M+1, \ldots) \\ 0 & (\text{Otherwise}) \end{cases}$$

This distribution is always skewed to the right, as illustrated in sketch B6.

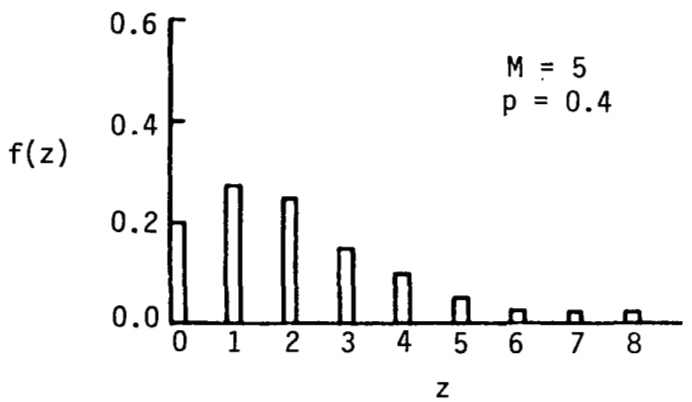

Sketch B6

The mean and variance are $M(1 - p)/p$ and $M(1 - p)/p^2$, respectively. Hence, the estimates based on the sample mean and variance are

$$M = \bar{z}^2/(s^2 - \bar{z})$$

and

$$p = \bar{z}/s^2$$

These estimates require that $s^2 > \bar{z}$ in order for M and p to be positive.

Poisson distribution.- The Poisson distribution (see sketch B7) is the limit of binomial distributions as n becomes infinite, p tends to zero, and the mean remains constant ($np = \lambda$). The probability density function (ref. 7) is

APPENDIX B

$$f(z) = \begin{cases} \lambda^z \exp(-\lambda)/z! & (z = 0, 1, 2, \ldots;\ \lambda > 0) \\ 0 & \text{(Otherwise)} \end{cases}$$

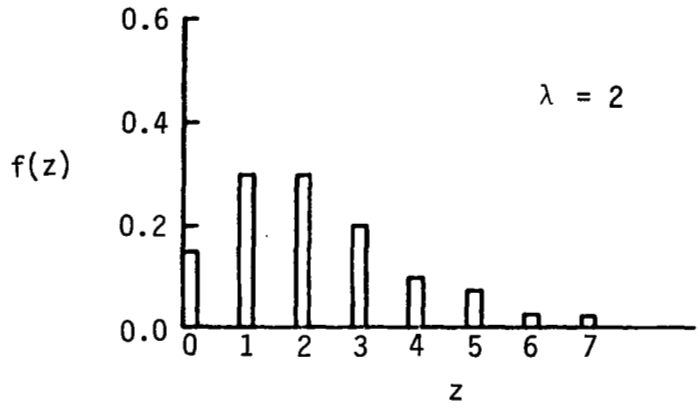

Sketch B7

This distribution is often used in queueing theory and in reliability theory where the event is an arrival at a waiting line or the failure of a machine, respectively. The random variable z is the number of events occurring in one unit of time.

The mean and the variance of the Poisson distribution are identical and are equal to λ. Therefore, this distribution applies if $\bar{z}$ and s^2 are approximately equal; λ may be estimated from $\bar{z}$ or s^2, or the average of $\bar{z}$ and s^2.

REFERENCES

1. Deloach, Richard: An Airport Community Noise-Impact Assessment Model. NASA TM-80198, 1980.

2. Credeur, Leonard; Davis, Christina M.; and Capron, William R.: Evaluation of Microwave Landing System (MLS) Effect on the Delivery Performance of a Fixed-Path Metering and Spacing System. NASA TP-1844, 1981.

3. Johnson, Norman L.; and Kotz, Samuel: Continuous Univariate Distributions-1. Houghton Mifflin Co., c.1970.

4. Lindgren, B. W.: Statistical Theory, Second ed. Macmillian Co., c.1968.

5. Tausworthe, Robert C.: Random Numbers Generated by Linear Recurrence Modulo Two. Math. Comput., vol. 19, no. 90, Apr. 1965, pp. 201-209.

6. Johnson, Norman L.; and Kotz, Samuel: Continuous Univariate Distributions-2. Houghton Mifflin Co., c.1970.

7. Johnson, Norman L.; and Kotz, Samuel: Discrete Distributions. Houghton Mifflin Co., c.1969.

SYMBOLS

a,b	coordinates of center of circle
A,B,C	points where alternate paths diverge
C1,...,C8	designators of curvilinear segments
d,e	lower and upper limits of uniform distribution
f(z)	probability density function of z
h	altitude, hundreds of feet (H on computer plots)
Δh	change in altitude along segment, hundreds of feet
h*	minimum altitude, hundreds of feet
h_0	initial aircraft altitude, hundreds of feet
ℓ	length of linear segment
$\Delta\ell$	increment to linear segment length
L1,...,L12	designators of linear segments
m	number of points generated along segment
M	negative binomial parameter
n	binomial parameter
N	number of flight paths generated from one runway
p	probability of success on one trial
r	radius of circle
r_0	criteria for distinguishing between curve and line; threshold radius
R	distance from initial point to arbitrary point on curve
s	sample standard deviation
s^2	sample variance
T	turn direction indicator (+1 is left, -1 is right)
x,y	Cartesian coordinates (X,Y on computer plots)
x_0,y_0	initial Cartesian coordinate of flight path
x',y'	Cartesian coordinate used to find turn direction
z	random variable

$\bar{z}$ sample mean

z^* minimum value of z in sample

z' log transform of $(z - \tau)$

α angle between x-axis and line segment, rad

θ turn angle, rad

$\Delta\theta$ increment to turn angle, rad

λ parameter of Poisson distribution

μ population mean

σ population standard deviation

τ threshold parameter of lognormal distribution

Ψ track angle, rad

Subscripts:

i index of segment parameters

j index of coordinates along segment

Abbreviation:

pdf probability density function

1. Report No.	2. Government Accession No.	3. Recipient's Catalog No.
NASA TP-1997		

4. Title and Subtitle	5. Report Date
ANALYSIS AND MONTE CARLO SIMULATION OF NEAR-TERMINAL AIRCRAFT FLIGHT PATHS	April 1982
	6. Performing Organization Code: 505-31-83-02
7. Author(s): James R. Schiess and Christine G. Matthews	8. Performing Organization Report No.: L-15062
	10. Work Unit No.
9. Performing Organization Name and Address: NASA Langley Research Center, Hampton, VA 23665	11. Contract or Grant No.
	13. Type of Report and Period Covered: Technical Paper
12. Sponsoring Agency Name and Address: National Aeronautics and Space Administration, Washington, DC 20546	14. Sponsoring Agency Code

15. Supplementary Notes

James R. Schiess: Langley Research Center.
Christine G. Matthews: Computer Sciences Corporation, Hampton, Virginia.

16. Abstract

This paper addresses the problem of stochastically representing the flight paths of arriving and departing aircraft at an airport. Radar data of the aircraft movements are used to decompose the flight paths into linear and curvilinear segments. Variables which describe the segments are derived and the best fitting probability distributions of the variables, based on a sample of flight paths, are found. Conversely, given information on the probability distribution of the variables, generation of a random sample of flight paths in a Monte Carlo simulation is discussed. The paper concludes with the analysis and simulation of actual flight paths at Dulles International Airport.

17. Key Words (Suggested by Author(s))	18. Distribution Statement
Probability distributions Ground tracks Analytic geometry Altitude profile	Unclassified - Unlimited Subject Category 04

19. Security Classif. (of this report)	20. Security Classif. (of this page)	21. No. of Pages	22. Price
Unclassified	Unclassified	38	A03

For sale by the National Technical Information Service, Springfield, Virginia 22161 NASA-Langley, 1982

National Aeronautics and
Space Administration

Washington, D.C.
20546

Official Business
Penalty for Private Use, $300

THIRD-CLASS BULK RATE

Postage and Fees Paid
National Aeronautics and
Space Administration
NASA-451

U.S. MAIL

U.S.A. 042082 S00903DS
DEPT OF THE AIR FORCE
AF WEAPONS LABORATORY
ATTN: TECHNICAL LIBRARY (SUL)
KIRTLAND AFB NM 87117

NASA

POSTMASTER: If Undeliverable (Section 158 Postal Manual) Do Not Return